Functional Redundancy of R7 RGS Proteins in ON-Bipolar Cell Dendrites

Frank S. Chen,[1] *Hoon Shim,*[1] *Duncan Morhardt,*[1] *Rebecca Dallman,*[1] *Elizabeth Krahn,*[1] *Ludine McWhinney,*[1] *Anjali Rao,*[1] *Stephen J. Gold,*[2,3,4] *and Ching-Kang Chen*[1]

Purpose. In the *Gβ5*$^{-/-}$ mouse, the electroretinogram (ERG) b-wave is absent, and the R7 subfamily of regulators of G protein signaling (RGS), which includes RGS6, -7, -9, and -11, is downregulated. Mutant mouse strains deficient in RGS7 or -11 were characterized, and the *SG711* strain which is deficient in both proteins was examined, to learn whether the loss of some of these RGS proteins causes the absence of the ERG b-wave.

Methods. Antibodies to RGS7 and -11 were generated to determine their expression levels and localizations in retinas with various genetic backgrounds by Western blot analysis and immunohistochemistry, respectively. The implicit times and amplitudes of ERG a- and b-waves were analyzed to examine photoreceptor and bipolar cell functions.

Results. RGS7 and -11 co-localized to the dendritic tips of the ON-bipolar cells. In the *RGS11*$^{-/-}$ mouse, the level of RGS7 protein increased. However, the level of RGS11 protein remained unchanged in the *RGS7* mutant mouse, where a truncated RGS7 protein was expressed due to the deletion of exon 10. In the *SG711* mouse retina, the Gβ5-S protein level was reduced. The ERG b-wave of SG711 mice was markedly delayed. In contrast, *RGS11*$^{-/-}$ mice showed a moderately delayed b-wave, whereas the *RGS7* mutant mice showed normal ERG responses.

Conclusions. The data demonstrate the presence of a delayed ERG b-wave in *SG711* mice and a functionally redundant role for RGS11 and -7 at the tips of ON-bipolar cell dendrites. These results suggest that RGS11 or -7 works as the major physiological GAP (GTPase acceleration protein) for Gαo1 in ON-bipolar cells. (*Invest Ophthalmol Vis Sci.* 2010;51:686–693) DOI: 10.1167/iovs.09-4084

Vision begins at retinal photoreceptors, and encoded information is relayed to bipolar cells at the retinal outer plexiform layer (OPL). The phototransduction cascade responsible for transducing light into neural signals in photoreceptors is G-protein mediated,[1] as is the metabotropic glutamate receptor 6 (mGluR6) signaling pathway responsible for relaying visual information in the depolarizing bipolar cells (DBCs).[2] In the outer segment of a rod photoreceptor, light activates rhodopsin, which in turn activates the photoreceptor-specific G-protein, transducin. Activated transducin sequesters the inhibitory subunit of a phosphodiesterase and in turn enables its catalytic subunits to hydrolyze cyclic guanosine monophosphate (cGMP), leading to a rapid decline in intracellular cGMP level and to the closure of cGMP-gated cation channels located in the plasma membranes of the outer segment. Channel closure leads to membrane hyperpolarization and decreases synaptic release of glutamate in the OPL. The reduction of glutamate concentration is sensed by dendrites of two types of bipolar cells. In hyperpolarizing bipolar cells (HBCs) ionotropic glutamate receptors are expressed and the cell becomes hyperpolarized in response to the light-induced decrease in OPL glutamate level. In contrast, mGluR6 is expressed in DBCs, and light exposure causes the cell to depolarize. An alternatively spliced form of Gαo, Gαo1, is necessary for DBC-derived ERG b-wave responses.[3,4] It is known that activation of mGluR6 by glutamate leads to the closure of a cation channel,[5] which has recently been suggested to be a transient receptor potential–like channel, TRPM1.[6] Akin to the knockout mouse deficient in mGluR6 or Gαo,[4,7] the *TRPM1*-knockout mouse lacks the ERG b-wave.[6] Unlike the phototransduction cascade, many components involved in the mGluR6 signaling pathway remain unidentified.

Recently, several RGS proteins, including RGS7, RGS11, and Ret-RGS1, were postulated to participate in the mGluR6 signaling pathway.[8–10] RGS functions inside a cell as a negative regulator of a subset of heterotrimeric G-proteins.[11] Members of the RGS protein family contain a conserved RGS domain roughly 120 amino acids in length and can be further classified into subgroups by their sizes as well as sequences outside the RGS domain. RGS9-1 was the first mammalian RGS protein identified to have a physiological function. It is essential for timely deactivation of transducin in photoreceptors in mice and humans.[12,13] RGS9-1 exists in complex with two other proteins: Gβ5-L (long-splice form of the fifth member of the G-protein β subunit) and RGS9 anchoring protein (R9AP).[14,15] Together, these three proteins form the transducin GTPase acceleration protein (GAP) complex, the level of which determines the duration of rhodopsin signaling in rods.[16] The stability of the transducin GAP complex depends on a unique interaction between Gβ5-L and the G protein γ–like (GGL) domain of RGS9-1.[12,17] Three additional RGS proteins contain the hallmark GGL domain: RGS6, -7, and -11. Together with RGS9, they constitute the R7 subfamily of RGS proteins.[11] Unlike RGS9-1, however, these three R7 RGS proteins interact with the short-splice form of Gβ5 (Gβ5-S), which is more broadly expressed in the nervous system.[18] In *Gβ5* knockout (*Gβ5*$^{-/-}$) mice, all four R7 RGS proteins are destabilized, and the ERG b-wave is absent.[8,19] In addition to the no-b-wave ERG phenotype, DBCs of *Gβ5*$^{-/-}$ mice exhibit unique dendritic

From the [1]Department of Biochemistry and Molecular Biology, Virginia Commonwealth University, Richmond, Virginia; and the Departments of [2]Psychiatry and [3]Medicine, University of Texas Southwestern Medical Center, Dallas, Texas.

[4]Present affiliation: Merck Research Labs, Rahway, New Jersey.

Supported by National Institutes of Health Grant EY013811 (CKC).

Submitted for publication June 3, 2009; revised July 10 and August 23, 2009; accepted September 9, 2009.

Disclosure: **F.S. Chen**, None; **H. Shim**, None; **D. Morhardt**, None; **R. Dallman**, None; **E. Krahn**, None; **L. McWhinney**, None; **A. Rao**, None; **S.J. Gold**, None; **C.-K. Chen**, None

Corresponding author: Ching-Kang Chen, Department of Biochemistry and Molecular Biology, Virginia Commonwealth University, Box 980614, 1101 E. Marshall Street, Richmond, VA 23298; cjchen@vcu.edu.

defects as the result of an arrest in the formation of the triadic ribbon synapses during OPL development. Transgenic restoration of Gβ5-L in rods of adult *Gβ5*$^{-/-}$ mice rescued neither the OPL morphologic defects nor the absent ERG b-wave, indicating that both phenotypes come from the loss of Gβ5-S downstream of the photoreceptors.[8] However, it remains uncertain whether a signaling defect in the mGluR6 signaling pathway or the reduced triadic ribbon synapses at the OPL, or both, causes the absence of ERG b-wave in *Gβ5*$^{-/-}$ mice. To gain further insight, we recorded ERG responses from mice carrying targeted mutations in both *RGS7* and *-11* genes. We found that RGS7 and -11 are co-localized at the tips of DBC dendrites and that both are involved in the generation of ERG b-waves in a functionally redundant manner. Because of the presence of a robust, though delayed ERG b-wave response when both RGS7 and -11 are mutated, our data suggest that OPL morphologic defects, rather than the prolonged mGluR6/Gαo1 signal transduction in DBCs, are the major contributing factor to the loss of ERG b-waves in *Gβ5*$^{-/-}$ mice.

Methods

Animals

RGS11 and -7 mutant mice, generated by homologous recombination by Lexicon Pharmaceuticals (The Woodlands, TX), are available from the Mutant Mouse Regional Resource Center. In targeting the *RGS11* gene, the first four exons were deleted. The homozygous *RGS11* knockout (*RGS11*$^{-/-}$) mouse has no detectable RGS11 protein and hence is a true null.[20] However, in the homozygous *RGS7* mutant mouse, the deletion of exon 10 resulted in the production of a transcript encoding a truncated RGS7 protein lacking amino acids S229-Q261. To distinguish it from a true null, we named the homozygous mutant *RGS7* line the *SG7* mouse. The individually targeted mouse strains are viable and fertile with no noticeable behavioral deficits. To generate the *SG711* mice which carry homozygous mutations in both the *RGS7* and *-11* genes, the F1 offspring derived from *RGS11*$^{-/-}$ and *SG7* mating were intercrossed. Genotyping of the *SG711* mice was performed by PCR using tail-snip DNA as templates with 60°C annealing temperature. The 190-bp PCR product of the wild-type *RGS11* allele was amplified with the primers SG11WT-f: 5′-AGT TAA GGG CAT TGG AGA CCG T and SG11WT-r: 5′-CCA AAG AAA CCG AAA GTG TGT TAG GG. A 750-bp PCR product of the mutant *RGS11* allele was obtained with the primers SGNeo3A: 5′-GCA GCG CAT CGC CTT CTA TC and SG11KO: 5′-CTT CCA ATA TCC ACC CTA GC. A mixture of three primers was used to genotype RGS7 locus: SGNeo3A, SG7-c: 5′-GAC AGT CAG TGC TCA AAC CC, and SG7WT: 5′-CCT ACA CCA GAA ACC AAG CC. The presence of 290- and 380-bp products indicated wild-type and targeted alleles, respectively. To generate mice in which cone photoreceptors were marked with EGFP, a transgenic construct called pGOP-EGFP, which contains a 5-kb mouse green opsin promoter amplified according to Akimoto et al.,[21] followed by a full-length EGFP cDNA and a 0.6-kb mouse protamine polyadenylation signal, was injected into the F1 embryos of C57BL6 x BALB/c mating. Six founder lines, GGFP1–6, were produced with varying degrees of EGFP expression and distribution in retinal cones. GGFP-5 was used in this study because of its high expression level in the retina. The GGFP mice were genotyped by PCR by the presence of a 750-bp product with the following primers at 58°C annealing temperature: GOP1.1: 5′-GAG ACA GTT TTC TAC AGC CT and EGFP-r: 5′-TTA CTT GTA CAG CTC GTC. The *Gβ5*$^{-/-}$ mouse has been described.[19] All animals used in the study were pigmented. All studies adhered to the ARVO Statement for the Use of Animals in Ophthalmic and Vision Research. Experimental procedures were performed in accordance with the rules and regulations of the NIH guidelines for research animals and approved by the institutional animal care and use committee of Virginia Commonwealth University.

Antibodies

A rabbit polyclonal antibody for RGS11 (VCU008) was raised against a synthetic peptide (CQSTPREPAATSSPEGADGE) coupled to keyhole limpet hemocyanin and the antibody was affinity purified on the corresponding peptide column (Yenzym, Burlingame, CA). Similarly, a rabbit polyclonal antibody for RGS7 (VCU015) was raised and purified against a synthetic peptide (CKTLTSKRLTSLVQS; GenScript, Piscataway, NJ). Rabbit anti-Gβ5 antibody CT-215 was graciously provided by Mel Simon (California Institute of Technology, Pasadena, CA).[18] Goat anti-RGS11 antibody was generously provided by Kirill Martemyanov (University of Minnesota, Minneapolis, MN).[20] Rabbit anti-RGS7 antibody 7RC-1 was kindly provided by William Simonds (National Institute of Diabetic and Digestive and Kidney Diseases, Bethesda, MD).[22] Rabbit anti-RGS7 antibody H-190 was purchased from Santa Cruz Biotechnology (Santa Cruz, CA); rabbit anti-RGS6 antibody IMG-554 from Imgenex (San Diego, CA); rabbit anti-GAPDH antibody from Cell Signaling Technologies (Danvers, MA); and HRP-conjugated secondary antibodies from Santa Cruz Biotechnology.

Immunohistochemistry

The eyeballs were enucleated immediately after the animals were killed by CO_2 inhalation. A small incision was made in the cornea, and the eyes were immersion fixed with 4% paraformaldehyde in 1× phosphate-buffered saline (PBS) at 4°C for 10 to 30 minutes. The short fixation time is crucial for OPL staining of RGS7 and Gβ5, as previously noted.[8,9] After removal of the cornea and lens, the resulting eye cups were cryoprotected in cold 30% sucrose in 1× PBS, embedded in a freezing medium (Triangle Biomedical Sciences, Durham, NC), and sectioned at −20°C at 20-μm thickness. The sections were blocked for 1 hour at room temperature with 10% goat serum and 0.3% Triton X-100 in 1× PBS (PBT) and incubated with rabbit primary antibodies at 1:100 dilution for 4 to 8 hours at room temperature. Alexa 563-conjugated goat anti-rabbit antibody (1:2000 dilution; Invitrogen, Carlsbad, CA) was used as a secondary antibody for protein localization. For co-localization studies using antibodies raised in rabbit, a rabbit IgG labeling kit (Zenon Tricolor, Z25360; Invitrogen) was used according to the manufacturer's instructions. Briefly, 1 μg of affinity-purified antibody was incubated with the labeling reagents in a molar ratio of 1:3 for 5 minutes at room temperature, then stopped by adding the blocking reagent and incubated for an additional 5 minutes. The entire mixture was adjusted with 10% goat serum in PBT and then used in staining with appropriate dilutions unique to each primary antibody. Extensive washing (five times, 30 minutes each) was performed to minimize the background signal. Fluorescent images were acquired with a confocal microscope at the shared EM and microscopy facility of the Department of Anatomy and Neurobiology, Virginia Commonwealth University (LSM510Meta; Carl Zeiss Microimaging, Thornwood, NY). Unmodified *.lsm files were archived and viewed in a separate computer (LSM Image Browser program; Carl Zeiss Microimaging). Images were then exported as *.tif files and opened in image-analysis software (Photoshop; Adobe, San Jose, CA) for cropping. No post hoc image processing, such as contrast and brightness adjustments, was performed during or after image acquisition.

Immunoblot Analysis

Retinal extracts (10 μg) were resolved by 12% SDS-PAGE and transferred onto nitrocellulose membranes. The membranes were blocked with 10% dry milk in TBST buffer containing 25 mM Tris (pH 7.5), 137 mM NaCl, and 0.05% Tween-20. For the detection of both forms of Gβ5, CT215 was used at 1:10,000 dilution. To detect RGS7, 7RC-1 or H-190 was used at 1:20,000 and 1:5,000 dilution, respectively. For RGS11, goat anti-RGS11 or VCU008 was used at 1:5000 and 1:2000 dilution, respectively. The anti-GAPDH antibody was used at 1:200,000 dilution and the GAPDH signal was used as an internal lane-loading control. Species-specific secondary antibodies were used at 1:25,000 dilution. The signal was detected by enhanced chemiluminescence with an extended-duration substrate kit (SuperSignal West Dura;

Thermo Fisher Scientific, Rockford, IL), and was captured and quantified using an imaging system with accompanying 1-D image-analysis software (IS440; Eastman Kodak, Rochester, NY).

Electroretinography

Before ERG recording, the mice were dark-adapted overnight. They were anesthetized with ketamine/xylazine (150/10 mg/kg; IP), and the pupils were dilated in the dark for a minimum of 10 minutes with topical eye drops of 1% tropicamide and 2.5% phenylephrine (Bausch & Lomb, Tampa, FL). The body temperature was monitored by a rectal probe (Braintree Scientific, Braintree, MA) and maintained at 35°C to 37°C using a plastic heating coil with 43.5°C circulating water. ERG from both eyes was recorded simultaneously (UTAS E-3000 system; LKC Technologies, Gaithersburg, MD) under scotopic conditions, as previously described.[23] Typically, the difference in a-wave amplitudes between the two eyes of an animal was <10%. For the study of light sensitivity, responses from 3 to 20 flashes were averaged at different flash intensities. The interstimulus interval (ISI) was changed incrementally from 5 to 180 seconds with increasing stimulus intensity to ascertain the dark-adapted state of the animals. For double-flash recordings, the interval between trials was empirically determined to be >120 seconds. A typical recording session lasted 2 to 3 hours, and booster injections of ketamine/xylazine (one fifth of the initial volume) were given subcutaneously as needed to maintain a steady plane of anesthesia. Because of the length of the recording period, 5 μL of filtered PBS was added every 20 minutes to the surface of the eyes to prevent corneal clouding and cataract formation.

Determination of the Amplification Factor of Rod Phototransduction

The amplification factor of rod phototransduction was determined in a data-analysis software (IgorPro; Wavemetrics, Lake Oswego, OR) by fitting the early descending portion of the ERG a-waves initiated by 0.02-, 0.16-, 0.4-, 0.93-, 2.4-, and 245-cd s m^{-2} white flashes to the following equation, according to the Lamb and Pugh[24] model: $A(x) = 1 - \exp[-0.5 \cdot p \cdot A \cdot (x - t)^2]$, where $A(x)$ is the fraction of a-wave amplitude at time x, A is the amplification factor, p is the bleaching efficiency empirically determined, and t is the latent time between flash onset and the start of the descending a-waves. The bleaching efficiency was determined spectrophotometrically by measuring rhodopsin content in a retinal homogenate derived from anesthetized and pupil-dilated animals sitting in the actual recording position in the Ganzfeld before (from the right eyes) and after (from the left eyes) 20 flashes of 684-cd s m^{-2} intensity delivered at 1 Hz. The average reduction in rhodopsin content induced by a single flash is 2.61% ± 0.43% (n = 20). The bleaching efficiency at weaker flashes was then calculated according to the calibration of the Ganzfeld performed by the manufacturer and by assuming 7×10^7 to be the average number of rhodopsin/rod[25] and the number of rods/retina to be 6.4×10^6, as described previously.[26] The conversion factor of 1 cd s m^{-2} to photoisomerization/rod/s is approximately 1400 under our experimental conditions.

Determination of the Pepperberg Constant

The recovery phase of rod phototransduction was determined by double-flash techniques as previously described.[27] The relationship between ISI (in milliseconds) and 1 - $R(t)/R_{max}$, where $R(t)$ is the a-wave amplitude when t = ISI and the R_{max} is the amplitude when ISI = 2000, was determined. The test (first) flash intensity ranged from −0.81, −0.4, −0.03, and 0.38 log cd s m^{-2} and the probe (second) flash intensity was fixed at 1.63. By plotting $1 - R(t)/R_{max}$ versus ISI and ensemble-fitting the data in the analysis software (IgorPro; Wavemetrics) using a customized exponential function: $f(x) = 1 - \exp\{-a \cdot \exp[(b - x)/t]\}$, where a is a coefficient, b is the time at which there is no recovery, and t is an exponential decay time constant, the time required for 50% recovery is determined for each of the four test flash intensities and used in the Pepperberg plot in which the ISI at 50% recovery (ordinate) vs. the natural log of photoisomerizations (R^*) per flash per rod per second (abscissa) was drawn. The slope of the linear regression line revealed the dominant recovery time constant (τ_D). The number of R^* produced in each test flash was calculated according to the empirically determined conversion factor.

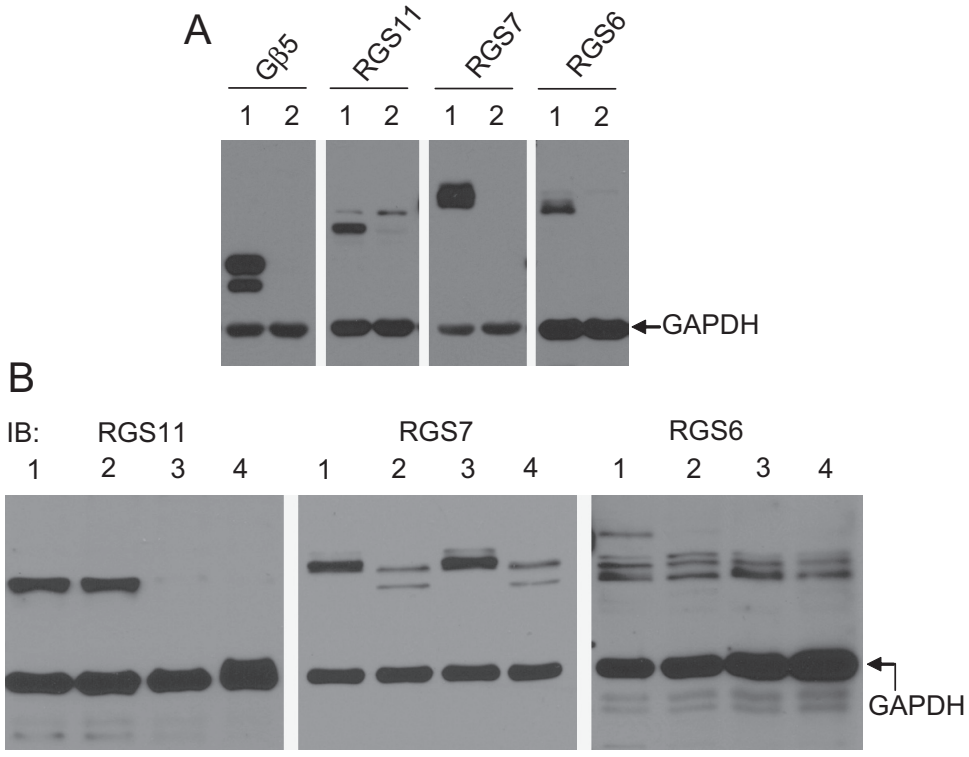

FIGURE 1. The level of R7 RGS proteins in retinas of various genetically modified mouse lines. (**A**) Western blot analysis of retinal extracts derived from wild-type (*lane 1*) and $G\beta5^{-/-}$ (*lane 2*) mice probed with the following antibodies: CT215 (anti-Gβ5), VCU008 (anti-RGS11), 7RC-1 (anti-RGS7), and IMG554 (anti-RGS6). (**B**) Western blot analysis showing the level of three R7 RGS proteins in retinal extracts derived from wild-type (*lane 1*), *SG7* (*lane 2*), $RGS11^{-/-}$ (*lane 3*), and *SG711* (*lane 4*) mice. *Arrows*: GAPDH signal used as an internal loading control.

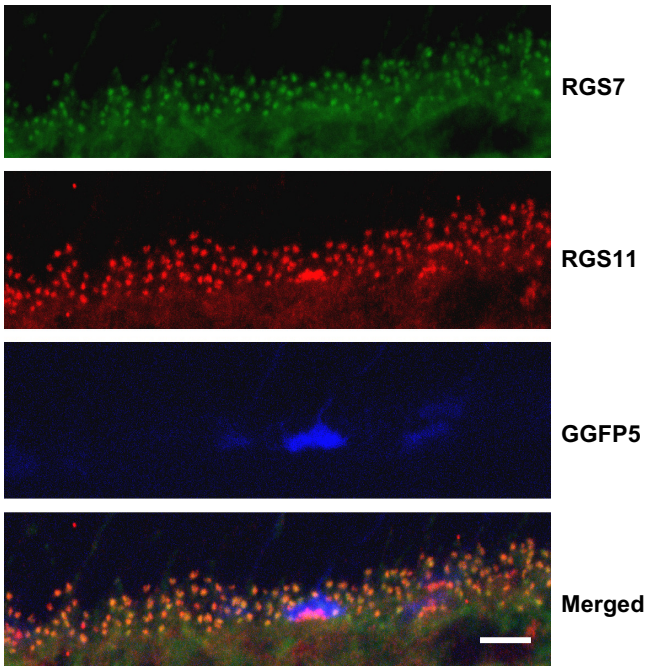

FIGURE 2. Co-localization of RGS7 and -11 at the tips of DBC dendrites. A maximum projection transformation of a 3.2-μm *z*-stacked confocal image of the OPL of a GGFP5 mouse retinal section is shown. The retinal section was stained with two rabbit polyclonal antibodies, H190 (anti-RGS7) and VCU008 (anti-RGS11), in conjunction with the rabbit IgG labeling kit. Most cone terminals in the GGFP5 retina are visible under direct EGFP fluorescence. Both RGS7 and -11 are expressed in dendritic tips of DBCs and virtually all tips express both proteins. Scale bar, 5 μm.

Statistical Analysis

Data are expressed as the mean ± SEM. Differences among the four genotypes were examined using one-way analysis of variance and mean differences between genotypes were analyzed by Tukey HSD test (JMP8 software ; SDS, Cary, NC). Differences were considered significant when $P < 0.05$.

RESULTS

Coexpression of RGS7 and -11 in the Dendritic Tips of DBCs

We and others have reported that RGS7 and -11 proteins localize to the tips of DBC dendrites.[8,9] However, the degree to which they co-localize in individual dendritic tips has not been assessed. Using the rabbit IgG labeling kit (Zenon; Invitrogen), we investigated the distribution patterns of RGS7 and -11 in retinal OPL using two well-characterized rabbit antibodies against RGS7 (7RC-1)[20,22] and RGS11 (VCU008, see the Methods section). The specificity of the two antibodies was verified by using retinal extracts derived from wild-type, *Gβ5*$^{-/-}$, and respective gene-targeted mice (Fig. 1). Immunofluorescence with these two antibodies revealed that RGS11 and -7 are co-localized to the tips of bipolar cell dendrites (Fig. 2). Because RGS7 and -11 both require interaction with Gβ5-S for stability,[19] the co-localization suggests a possible redundant function for these two R7 RGS proteins at the tips of DBC dendrites.

Upregulation of RGS7 in the RGS11 Knockout Retinas

Because the localization of RGS7 and -11 overlaps in the OPL, we examined how the level of each RGS proteins is influenced by the targeted mutation of the other. As seen in Figure 3, whereas the overall concentration of Gβ5-S remained unchanged in the *RGS11*$^{-/-}$ retinal extracts, the RGS7 level increased an average of 60% in the *RGS11*$^{-/-}$ mice. In contrast, we did not observe detectable changes in the RGS11 level in the *SG7* mice (Fig. 1B). The changes in RGS7 levels were specific because the level of RGS6 was not affected in either the *RGS11*$^{-/-}$ or the *SG7* mice, even though, similar to other R7 RGS members, it was downregulated below detection level in the *Gβ5*$^{-/-}$ mice (Fig. 1A). These data support a selective, compensatory upregulation of RGS7 in retinas of *RGS11*$^{-/-}$ mice, which would be predicted for proteins with redundant functions. Failure to observe an increase in RGS11 in *SG7* mice may be explained by the incomplete genetic knockout in SG7 mice.

The Decrease of Gβ5-S Level in the SG711 Mice

RT-PCR analysis of RNA derived from homozygous *RGS7* mutant mouse retinas revealed *RGS7* transcripts with exon-10 deletion, which leads to a loss of 33 amino acids (S229-Q261) with the first 27 residues in the interdomain and the last 6 residues in the GGL domain required for interaction with Gβ5-S. This truncated RGS7 protein was not stable when ectopically expressed in insect H5 cells (data not shown). However, in the retina, the truncated RGS7 were detectable and appeared as multiple bands in the immunoblots (Figs. 1, 4). Most of the truncated RGS7 bands migrate faster than the wild-type RGS7 when longer electrophoretic time was used

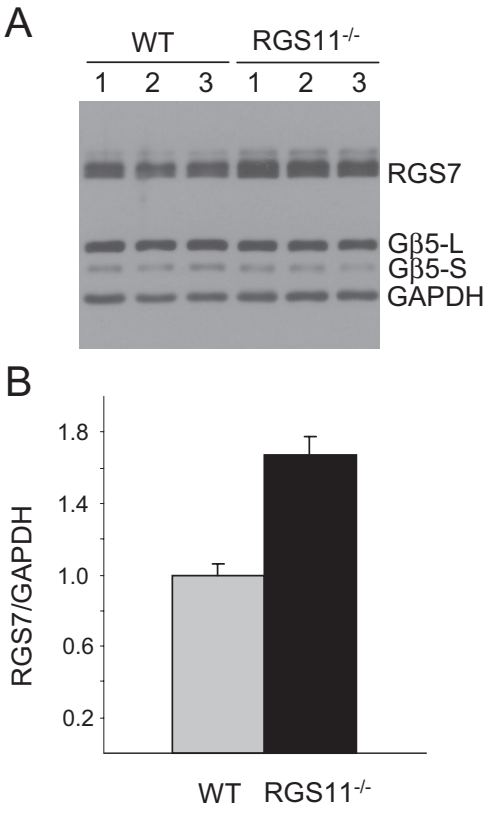

FIGURE 3. Upregulation of RGS7 level in *RGS11*$^{-/-}$ mouse retinas. (**A**) A representative immunoblot showing RGS7, Gβ5 spliced forms, and GAPDH levels in wild-type (WT) and *RGS11*$^{-/-}$ mouse retinas. (**B**) Quantification of RGS7 signal strength as normalized to the level of GAPDH between the two genotypes. The levels of Gβ5-L and -S are similar (data not shown) but a significant increase in RGS7 level is apparent ($n = 6$).

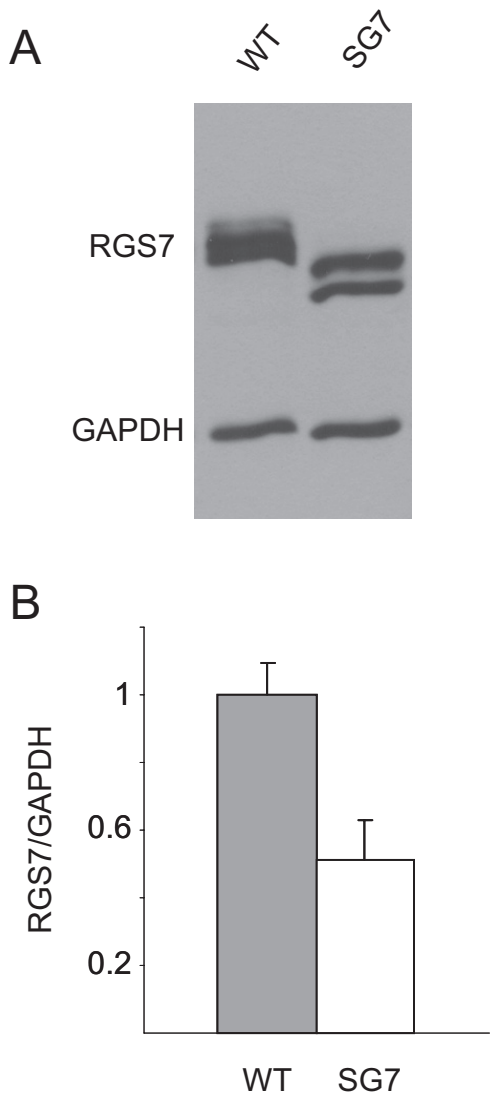

FIGURE 4. Exon10 deletion of *RGS7* reduced both the size and the level of RGS7 in *SG7* mouse retinas. (**A**) A representative immunoblot showing the level of the truncated mutant RGS7 protein in *SG7* versus WT mouse retinas. (**B**) Quantification of the level of reduction in RGS7 using GAPDH signal as a normalization factor ($n = 8$). A significant 50% decrease of overall RGS7 level was found in the *SG7* retinas, whereas the level of RGS11 remained unchanged (data not shown).

(Fig. 4). We have frequently obtained more than one band of RGS7 by immunoblots, and similarly we have found more than one RGS7 transcript by RT-PCR. The relationship between the multiple transcripts and the proteins is still under investigation. To compare the levels of the normal and mutant RGS7 in wild-type and *SG7* mice, we took into account the ensemble signals from all bands and found an average 50% reduction in the level of truncated RGS7 in *SG7* mice when compared with full-length RGS7 in wild-type, suggesting that the mutant RGS7 protein is also less stable in the retina. These results did not depend on the nature of the antibody used since similar results were obtainable with an independent, commercially available RGS7 antibody, H-190, and a custom-made antibody named VCU015, which targets a C-terminal peptide of mouse RGS7 (data not shown). Thus, these results support the conclusion that RGS7 is an unstable, truncated protein in retinas of *SG7* mice.

We next examined how the level of retinal Gβ5-S protein changes when both *RGS7* and *-11* genes are targeted. Figure 5 shows that the Gβ5-S protein level decreased by ~30% in *SG711* mice. However, the reduction of Gβ5-S in the *SG711* retina is not the result of the elimination of Gβ5-S in the OPL as it can still be found at the dendritic tips of DBCs in *SG711* mice (data not shown). We reason that the truncated RGS7 protein lacking S229 to Q261 can still weakly associate with Gβ5-S to protect it from degradation.

Comparable Phototransduction Properties in the Control and Mutant R7 RGS Mice

The abundant expressions of all members of R7 RGS proteins in the retina indicate their involvement in various retinal responses. To assess whether the loss of RGS11 protein or the truncation of RGS7 protein affects phototransduction, we recorded and analyzed ERG a-waves from these mice and determined the two major photoreceptor-derived properties, the amplification factor[24] and the dominant recovery time constant[27] (Table 1). We found similar maximum a-wave amplitude, amplification factor, and dominant recovery time constant (the Pepperberg constant) among the different genotypes. Therefore, we conclude that photoreceptor functions are normal when both *RGS7* and *-11* are targeted. This finding is consistent with the fact that RGS9-1 is the major R7 RGS protein in photoreceptors.[12,16,28]

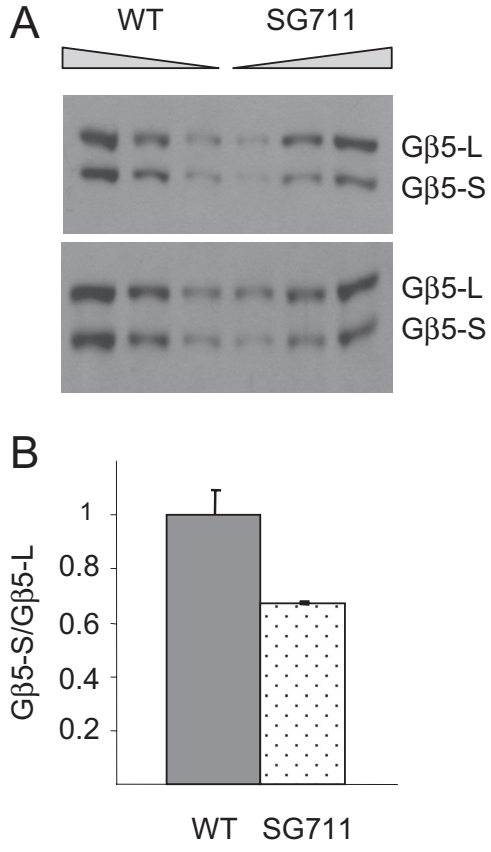

FIGURE 5. Downregulation of Gβ5-S in *SG711* mouse retinas. (**A**) Representative immunoblots showing the level of Gβ5-S and -L in serially diluted retinal extracts (10, 5, and 2.5 μg protein/well from high to low) derived from WT and *SG711* mice. (**B**) Quantification of Gβ5-S versus Gβ5-L signals between WT and *SG711* mice ($n = 8$). A significant ~30% decrease in Gβ5-S level is found in *SG711* mice.

TABLE 1. Properties of ERG a- and b-Waves in Different Genotypes

	Wild-Type	*SG7*	*RGS11*$^{-/-}$	*SG711*
a-Wave amplitude, μV*	451 ± 54 (n = 8)†	510 ± 25 (n = 6)	513 ± 62 (n = 8)	433 ± 67 (n = 10)
$A(S^{-2})$‡	15.3 ± 1.5 (n = 8)	15.6 ± 1.7 (n = 6)	16.1 ± 1.8 (n = 8)	13.9 ± 2.1 (n = 10)
τ_D, ms§	189 ± 12 (n = 17)	200 ± 9 (n = 6)	175 ± 8 (n = 8)	193 ± 8 (n = 8)
b-Wave implicit time, ms‖	65.9 ± 3 (n = 15)	67.8 ± 2.9 (n = 8)	84.7 ± 3.4 (n = 13)¶	113.7 ± 8.7 (n = 10)#
b-Wave amplitude, μV	870.9 ± 38.7 (n = 15)	946.4 ± 50.6 (n = 8)	881.9 ± 84.8 (n = 13)	925.5 ± 85.6 (n = 10)

* Elicited by a flash intensity of 245 cd s m^{-2}.

† Mean ± SEM (sample size).

‡ The amplification factor of phototransduction, obtained by curve-fitting the descending arms of a-waves according to the Lamb and Pugh[24] model.

§ The dominant recovery time constant determined by Pepperberg plots.

‖ Elicited by 89-cd sec m^{-2} flash intensity, represented by the bottom traces in Figure 6.

¶ $P < 0.05$ as compared to wild-type; Tukey HSD test.

# $P < 0.05$ as compared to wild-type, *SG7*, and *RGS11*$^{-/-}$; Tukey HSD test.

Prolonged ERG b-Wave Implicit Time in the RGS11$^{-/-}$ and SG711 Mice

Despite the normal photoreceptor functions, we noticed a clear difference in ERG responses between the control, *RGS11*$^{-/-}$, and *SG711* mice. The ERG b-wave implicit time significantly increased in the *RGS11*$^{-/-}$ and *SG711* mice, whereas the overall b-wave amplitudes remained similar among the four genotypes (Figs. 6, 7; Table 1). Notably, the rise time of the ERG b-wave in the *RGS11*$^{-/-}$ mice was delayed at all flash intensities tested when compared with the wild-type control (Fig. 7A). In addition, further delays in the ERG b-wave implicit time were observed in the *SG711* mice, especially when flash strength was above 1 cd s m^{-2}, an intensity that elicits mixed rod/cone responses (Fig. 7A). Because we found

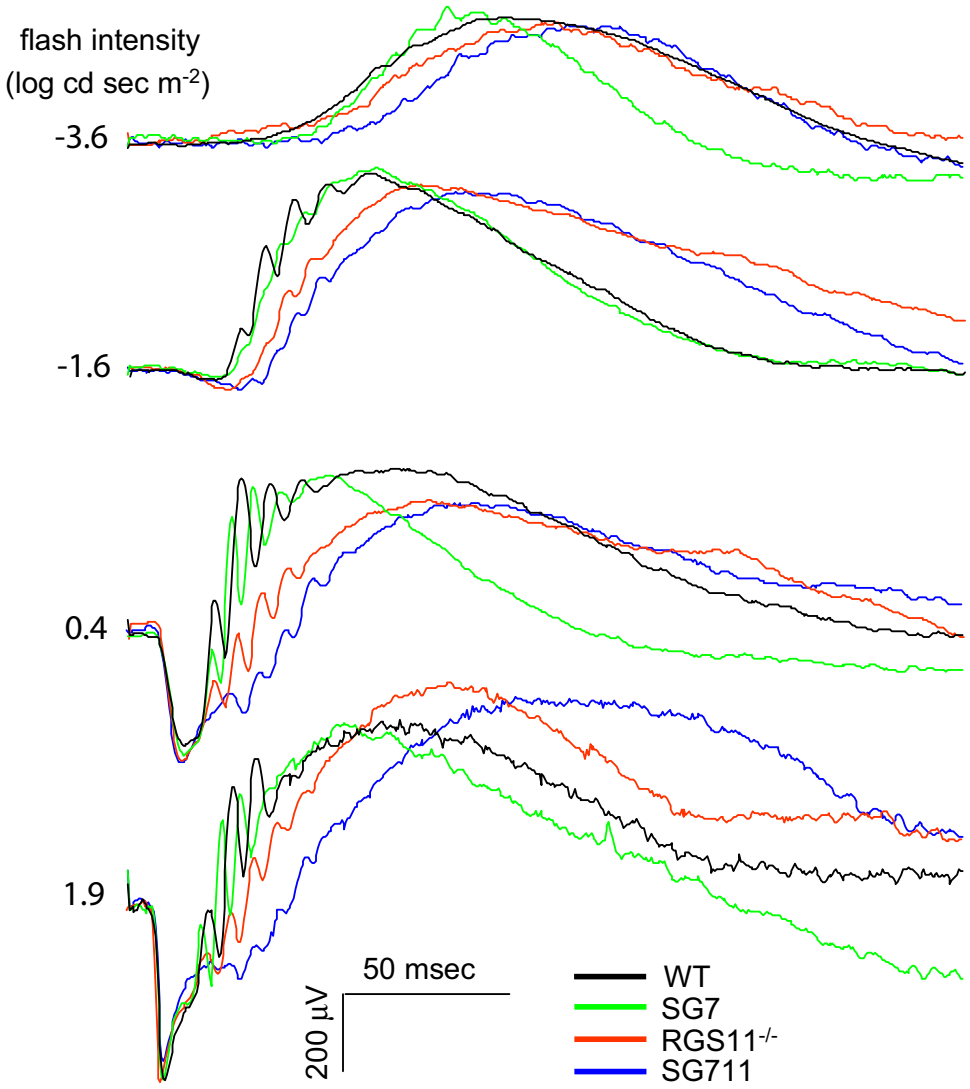

FIGURE 6. Delayed ERG b-wave in *RGS11*$^{-/-}$ and *SG711* mice. Representative scotopic ERG responses from the four genotypes are shown. Flash intensity is indicated at *left* (in log cd s m^{-2}).

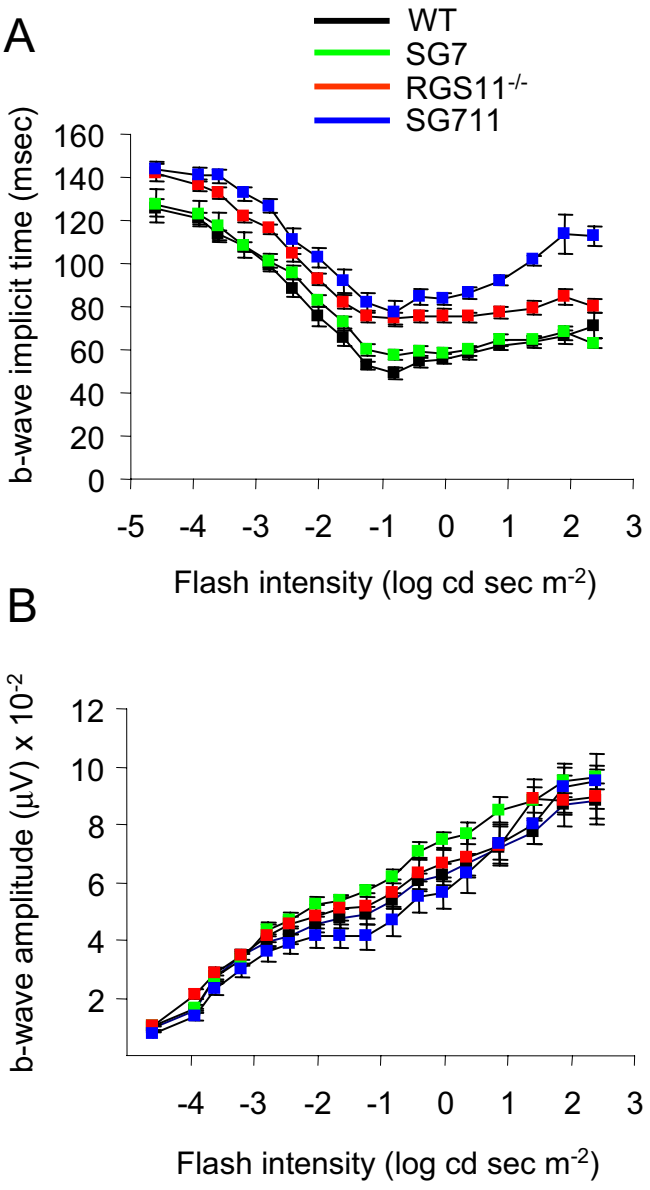

FIGURE 7. Measurement of ERG b-wave implicit time (**A**) and amplitude (**B**) as a function of flash intensity in mice of different genotypes. WT: $n = 15$; *SG7*: $n = 8$; *RGS11*$^{-/-}$: $n = 13$; and *SG711*: $n = 10$. No difference between WT and *SG7* responses was found, although significantly larger b-wave implicit time (the time between flash onset and the peak of the b-wave) was present in the *SG711* and *RGS11*$^{-/-}$ mice, compared with the WT control mice.

no differences between the control and *SG7* mice but found clear differences between the control, *RGS11*$^{-/-}$, and *SG711* mice, the increased ERG b-wave implicit time suggests that RGS7 is functionally redundant to RGS11 and both are involved in the generation of normal mouse ERG b-waves.

DISCUSSION

The deletion of exon 10 of the *RGS7* gene in the *SG7* mouse results in the expression of a truncated RGS7 protein instead of a null. Using this *SG7* line to understand RGS7 function has both advantages and shortcomings. First, by mapping the deleted residues to those of RGS9-1, whose crystal structure is known,[29] we found that the deletion spans an upstream linker region and the first six residues of the GGL domain. This deletion may affect GGL domain function, which is essential for Gβ5 interaction and protein stability.[17,19] Second, we found that the truncated RGS7 protein is less stable with approximately 50% of the wild-type level in retinas of *SG7* mice (Fig. 4). Together, these data suggest that deletion of the 33 amino acids results in a partial loss-of-function RGS7 protein in vivo. This loss-of-function hypothesis is consistent with the measurable behavioral phenotypes of *SG7* mice (available online from the Jackson Laboratory, Bar Harbor, ME at http://www.informatics.jax.org/external/ko/lexicon/1011.html), which includes hypoactivity and decreased exploratory responses in the open field. Of interest, *RGS11*$^{-/-}$ mice show no phenotype in the open-field test.

The shortcoming of using a partial loss-of-function mutant such as the *SG7* mouse is that the incomplete deletion limits the conclusions that can be drawn regarding the role of RGS7. For example, we found that *SG711* mice generated in this study do not exhibit an obvious weight defect during early postnatal development (data not shown) as reported for *Gβ5*$^{-/-}$ mice.[19] Because the *SG7* mouse is not a null, we cannot conclude whether the weight defects of *Gβ5*$^{-/-}$ mice are the consequence of simultaneous loss of RGS7 and -11. Similarly, we find it difficult to determine the exact contribution of RGS7 in the generation of ERG b-wave because there is no significant difference in response kinetics between *SG7* and control mice. Therefore, efforts to generate and characterize a true *RGS7* null mouse line are necessary for a firmer understanding of RGS7 function. Despite this gap, the significant differences in ERG responses in *RGS11*$^{-/-}$ and *SG711* mice when compared with control mice (Figs. 6, 7) strongly support the involvement of both RGS11 and -7 in the generation of a normal ERG b-wave.

Functional Redundancy of RGS7 and -11

We and others have reported the expression of various RGS proteins including RGS7, RGS11, and Ret-RGS1 in DBCs.[8–10] The lack of an ERG b-wave in *Gβ5*$^{-/-}$ mice, in which all R7 RGS proteins are downregulated, suggests that Gβ5-S/RGS7 and Gβ5-S/RGS11 may be the physiological GAP for Gαo1 in DBCs. We found that RGS7 and -11 coexist at the OPL (Fig. 2), pointing to functional redundancy of these two proteins at the tips of DBC dendrites. Because both RGS7 and -11 depend on their interaction with Gβ5-S for stability, one would expect a compensatory change in protein levels when either RGS is inactivated. Indeed, we found that the RGS7 protein level increased significantly in the *RGS11*$^{-/-}$ retina (Figs. 1, 3). Unfortunately, we could not test the converse, because the *SG7* mouse is not a null. Despite this limitation, we provide strong support for functional redundancy between RGS7 and -11 in the ERG responses of these mice. The ERG b-wave responses of *RGS11*$^{-/-}$ and *SG711* mice showed a significantly delayed rise time, even though the *SG7* mice showed no difference from the WT controls. Furthermore, our data suggest that RGS11 is the major RGS protein in the dendritic tips of DBCs because the delay in ERG b-wave is seen at all flash intensities tested in *RGS11*$^{-/-}$ mice, despite a compensatory increase in RGS7 (Figs. 1, 3).

Mechanism of RGS Modulation of ERG b-Wave

In the dark, mGluR6 at the dendritic tips of DBCs is nearly saturated by glutamate[30] and the ERG b-wave reflects the light-induced reopening of cation channels in DBCs.[31] Thus, the observed increase in implicit time of the ERG b-wave of *RGS11*$^{-/-}$ mice suggests a defect in the shutoff phase of the mGluR6/Gαo1 signaling pathway in DBCs. This unique ERG phenotype was further augmented in *SG711* mice (Figs. 6, 7), in which only the truncated and partial loss-of-function RGS7

protein was present in the OPL. Because mutant RGS7 by itself had no effect, but exacerbated the effect of *RGS11* inactivation on ERG b-wave responses, we conclude that both RGS7 and -11 are involved in the mGluR6/Gαo1 signaling pathway in DBCs and that they each function in the deactivation of Gαo1. However, it is noteworthy that the time course of the ERG b-wave in *SG711* mice (in milliseconds) was still much faster than the GTP turnover rate of Gαo1 (in seconds) assayed in vitro. Because several members of the RGS family are capable of accelerating GTP hydrolysis by Gαo1 in vitro,[10,17,32] the specific impact of RGS7 and/or -6 proteins on Gαo1 deactivation in DBCs and the possible involvement of other non-R7 RGS proteins require further investigation, which could be performed by examining the ERG responses of a true RGS7 null mouse individually or in combination with other relevant RGS knockout mice. Although an explanation for the missing ERG b-wave in $G\beta5^{-/-}$ mice remains elusive, this study clearly identified an overlapping expression pattern of RGS7 and -11 at the OPL and altered ERG responses in $RGS11^{-/-}$ and *SG711* mice. Together, these data firmly establish a redundant involvement of RGS7 and -11 in light-evoked responses of retinal ON-bipolar cells.

Acknowledgments

The authors thank Linda Boland, Lane Brown, and Catherine Morgans for critical reading of the manuscript. The GGFP transgenic mouse was generated in the transgenic mouse core facility at VCU.

References

1. Chen CK. The vertebrate phototransduction cascade: amplification and termination mechanisms. *Rev Physiol Biochem Pharmacol.* 2005;154:101–121.
2. Snellman J, Kaur T, Shen Y, Nawy S. Regulation of ON bipolar cell activity. *Prog Retin Eye Res.* 2008;27:450–463.
3. Dhingra A, Jiang M, Wang TL, et al. Light response of retinal ON bipolar cells requires a specific splice variant of Galpha(o). *J Neurosci.* 2002;22:4878–4884.
4. Dhingra A, Lyubarsky A, Jiang M, et al. The light response of ON bipolar neurons requires Gαo. *J Neurosci.* 2000;20:9053–9058.
5. Lasansky A. Properties of depolarizing bipolar cell responses to central illumination in salamander retinal slices. *Brain Res.* 1992; 576:181–196.
6. Shen Y, Heimel JA, Kamermans M, Peachey NS, Gregg RG, Nawy S. A transient receptor potential-like channel mediates synaptic transmission in rod bipolar cells. *J Neurosci.* 2009;29:6088–6093.
7. Masu M, Iwakabe H, Tagawa Y, et al. Specific deficit of the ON response in visual transmission by targeted disruption of the mGluR6 gene. *Cell.* 1995;80:757–765.
8. Rao A, Dallman R, Henderson S, Chen CK. Gbeta5 is required for normal light responses and morphology of retinal ON-bipolar cells. *J Neurosci.* 2007;27:14199–14204.
9. Morgans CW, Wensel TG, Brown RL, Perez-Leon JA, Bearnot B, Duvoisin RM. Gbeta5-RGS complexes co-localize with mGluR6 in retinal ON-bipolar cells. *Eur J Neurosci.* 2007;26:2899–2905.
10. Dhingra A, Faurobert E, Dascal N, Sterling P, Vardi N. A retinal-specific regulator of G-protein signaling interacts with Galpha(o) and accelerates an expressed metabotropic glutamate receptor 6 cascade. *J Neurosci.* 2004;24:5684–5693.
11. Ross EM, Wilkie TM. GTPase-activating proteins for heterotrimeric G proteins: regulators of G protein signaling (RGS) and RGS-like proteins. *Annu Rev Biochem.* 2000;69:795–827.
12. Chen CK, Burns ME, He W, Wensel TG, Baylor DA, Simon MI. Slowed recovery of rod photoresponse in mice lacking the GTPase accelerating protein RGS9-1. *Nature.* 2000;403:557–560.
13. Nishiguchi KM, Sandberg MA, Kooijman AC, et al. Defects in RGS9 or its anchor protein R9AP in patients with slow photoreceptor deactivation. *Nature.* 2004;427:75–78.
14. Watson AJ, Aragay AM, Slepak VZ, Simon MI. A novel form of the G protein beta subunit Gbeta5 is specifically expressed in the vertebrate retina. *J Biol Chem.* 1996;271:28154–28160.
15. Hu G, Wensel TG. R9AP, a membrane anchor for the photoreceptor GTPase accelerating protein, RGS9-1. *Proc Natl Acad Sci U S A.* 2002;99:9755–9760.
16. Krispel CM, Chen D, Melling N, et al. RGS expression rate-limits recovery of rod photoresponses. *Neuron.* 2006;51:409–416.
17. Snow BE, Krumins AM, Brothers GM, et al. A G protein gamma subunit-like domain shared between RGS11 and other RGS proteins specifies binding to Gbeta5 subunits. *Proc Natl Acad Sci U S A.* 1998;95:13307–13312.
18. Watson AJ, Katz A, Simon MI. A fifth member of the mammalian G-protein beta-subunit family: expression in brain and activation of the beta 2 isotype of phospholipase C. *J Biol Chem.* 1994;269: 22150–22156.
19. Chen CK, Eversole-Cire P, Zhang H, et al. Instability of GGL domain-containing RGS proteins in mice lacking the G protein beta-subunit Gbeta5. *Proc Natl Acad Sci U S A.* 2003;100:6604–6609.
20. Cao Y, Song H, Okawa H, Sampath AP, Sokolov M, Martemyanov KA. Targeting of RGS7/Gbeta5 to the dendritic tips of ON-bipolar cells is independent of its association with membrane anchor R7BP. *J Neurosci.* 2008;28:10443–10449.
21. Akimoto M, Filippova E, Gage PJ, Zhu X, Craft CM, Swaroop A. Transgenic mice expressing Cre-recombinase specifically in M- or S-cone photoreceptors. *Invest Ophthalmol Vis Sci.* 2004;45:42–47.
22. Rojkova AM, Woodard GE, Huang TC, Combs CA, Zhang JH, Simonds WF. Ggamma subunit-selective G protein beta 5 mutant defines regulators of G protein signaling protein binding requirement for nuclear localization. *J Biol Chem.* 2003;278:12507–12512.
23. Li S, Chen D, Sauve Y, McCandless J, Chen YJ, Chen CK. Rhodopsin-iCre transgenic mouse line for Cre-mediated rod-specific gene targeting. *Genesis.* 2005;41:73–80.
24. Pugh EN Jr, Lamb TD. Amplification and kinetics of the activation steps in phototransduction. *Biochim Biophys Acta.* 1993;1141: 111–149.
25. Lyubarsky AL, Daniele LL, Pugh EN Jr. From candelas to photoisomerizations in the mouse eye by rhodopsin bleaching in situ and the light-rearing dependence of the major components of the mouse ERG. *Vision Res.* 2004;44:3235–3251.
26. Jeon CJ, Strettoi E, Masland RH. The major cell populations of the mouse retina. *J Neurosci.* 1998;18:8936–8946.
27. Lyubarsky AL, Pugh EN Jr. Recovery phase of the murine rod photoresponse reconstructed from electroretinographic recordings. *J Neurosci.* 1996;16:563–571.
28. Krispel CM, Chen CK, Simon MI, Burns ME. Prolonged photoresponses and defective adaptation in rods of Gbeta5−/− mice. *J Neurosci.* 2003;23:6965–6971.
29. Cheever ML, Snyder JT, Gershburg S, Siderovski DP, Harden TK, Sondek J. Crystal structure of the multifunctional Gbeta5-RGS9 complex. *Nat Struct Mol Biol.* 2008;15:155–162.
30. Sampath AP, Rieke F. Selective transmission of single photon responses by saturation at the rod-to-rod bipolar synapse. *Neuron.* 2004;41:431–443.
31. Stockton RA, Slaughter MM. B-wave of the electroretinogram: a reflection of ON bipolar cell activity. *J Gen Physiol.* 1989;93:101–122.
32. Hooks SB, Waldo GL, Corbitt J, Bodor ET, Krumins AM, Harden TK. RGS6, RGS7, RGS9, and RGS11 stimulate GTPase activity of Gi family G-proteins with differential selectivity and maximal activity. *J Biol Chem.* 2003;278:10087–10093.